

# Azimuthal asymmetries in lepton-pair production at a fixed-target experiment using the LHC beams (AFTER)

Tianbo Liu<sup>1</sup>, Bo-Qiang Ma<sup>a,1,2</sup>

<sup>1</sup>School of Physics and State Key Laboratory of Nuclear Physics and Technology, Peking University, Beijing 100871, China

<sup>2</sup>Center for High Energy Physics, Peking University, Beijing 100871, China

Received: date / Accepted: date

**Abstract** A multi-purpose fixed-target experiment using the proton and lead-ion beams of the LHC was recently proposed by Brodsky, Fleuret, Hadjidakis and Lansberg, and here we concentrate our study on some issues related to the spin physics part of this project (referred to as AFTER). We study the nucleon spin structure through  $pp$  and  $pd$  processes with a fixed-target experiment using the LHC proton beams, for the kinematical region with 7 TeV proton beams at the energy in center-of-mass frame of two nucleons  $\sqrt{s} = 115$  GeV. We calculate and estimate the  $\cos 2\phi$  azimuthal asymmetries of unpolarized  $pp$  and  $pd$  dilepton production processes in the Drell–Yan continuum region and at the  $Z$ -pole. We also calculate the  $\sin(2\phi - \phi_S)$ ,  $\sin(2\phi + \phi_S)$  and  $\sin 2\phi$  azimuthal asymmetries of  $pp$  and  $pd$  dilepton production processes with the target proton and deuteron longitudinally or transversally polarized in the Drell–Yan continuum region and around  $Z$  resonances region. We conclude that it is feasible to measure these azimuthal asymmetries, consequently the three-dimensional or transverse momentum dependent parton distribution functions (3dPDFs or TMDs), at this new AFTER facility.

## 1 Introduction

Recently a multi-purpose fixed-target experiment using the proton and lead-ion beams of the Large Hadron Collider (LHC) extracted by a bent crystal, referred to as AFTER in the following, was proposed by Brodsky, Fleuret, Hadjidakis and Lansberg [1]. Such an extraction mode will not alter the performance of the collider experiments at the LHC. The center-of-mass energy is  $\sqrt{s_{NN}} = 115$  GeV with the LHC-7 TeV proton beam and  $\sqrt{s_{NN}} = 72$  GeV with the a lead running with 2.76 TeV-per-nucleon beam, and it can be even

higher by using the Fermi motion of the nucleons in a nuclear target. This project will provide a unique opportunity to study the nucleon partonic structure, spin physics, nuclear matter properties, deconfinement in heavy ion collisions,  $W$  and  $Z$  productions, exclusive, semi-exclusive and backward reactions, and even further potentialities of a high-energy fixed target set-up. We concentrate our study on some issues related to the spin physics for the AFTER proposal.

The study of the three-dimensional or the intrinsic transverse momentum dependent distribution functions (3dPDFs or TMDs) has received much attention in recent years [2]. Such new quantities of the nucleon provide us a significant perspective on understanding the three-dimensional structure of hadrons and the non-perturbative properties of quantum chromodynamics (QCD). The intrinsic transversal momentum of partons may cause special effects in high energy scattering experiments [3]. Azimuthal asymmetries of unpolarized and single polarized Drell–Yan processes are among the most challenging issues of QCD spin physics [4–6].

The first measurement of the angular distribution of Drell–Yan process, performed by NA10 Collaboration for  $\pi N$ , indicates a sizable  $\cos 2\phi$  azimuthal asymmetry [7, 8] which cannot be described by leading and next-to-leading order perturbative QCD [9]. Furthermore, the violation of the Lam–Tung relation [10] which is obtained from the spin-1/2 nature of quarks and the spin-1 nature of gluons, just like the Callan–Gross relation in the deep-inelastic scattering [11], was measured by Fermilab E615 Collaboration [12]. This violation was also tested by E866/NuSea Collaboration through the  $pd$  and  $pp$  Drell–Yan dimuon processes in recent year [13, 14].

Large single spin asymmetries (SSAs) were observed experimentally in the process  $pp^\uparrow \rightarrow \pi X$  two decades ago [15–20]. SSAs in semi-inclusive deeply inelastic scattering (SIDIS) [21–27] with one colliding nucleon transversely polarized have also been measured by several experiments. Standard per-

<sup>a</sup>e-mail: mabq@pku.edu.cn

turbative QCD based on collinear factorization to leading twist failed to explain these asymmetries [28].

The Drell–Yan process is an ideal ground for testing the perturbative QCD and for probing the 3dPDFs or TMDs, as it contains only the distribution functions with no fragmentation functions, and its differential cross section is well described by next-to-leading order QCD calculations [29]. In this paper, we calculate azimuthal asymmetries of  $pp$  and  $pd$  dilepton production processes in Drell–Yan continuum region and around the  $Z$ -pole through a fixed-target experiment using the LHC proton beams with the proton or deuteron target unpolarized and transversally or longitudinally polarized. The paper is organized as follows. In Sect. 2 and 3, we respectively calculate the azimuthal asymmetries in unpolarized and single polarized  $pp$  and  $pd$  processes. In Sect. 4, we present the numerical results of these asymmetries. Then, a brief discussion and conclusion is contained in Sect. 5.

## 2 The $\cos 2\phi$ azimuthal asymmetries of unpolarized $pp$ and $pd$ processes

The Drell–Yan process is an ideal ground to investigate the hadron structure, because it only probes the parton distributions without fragmentation functions. It was naively speculated that the polarization of at least one incoming hadron is necessary to investigate the spin-related structure and properties of hadrons. However, it is not the case if we take the intrinsic transversal momentum of quarks inside the hadron into account. As mentioned before, the standard perturbative QCD to leading and next-to-leading order failed to describe the sizable  $\cos 2\phi$  azimuthal asymmetry and the Lam–Tung relation violation of the unpolarized Drell–Yan experiments [7, 8, 12–14]. Several attempts were made to interpret this asymmetry, such as the factorization breaking QCD vacuum effect [9] (which corresponds possibly the helicity flip in the instanton model [30]), higher twist effect [31–33] and the coherent states [34]. Boer pointed out that the  $\cos 2\phi$  azimuthal asymmetry could be due to a non-vanished 3dPDF or TMD  $h_1^\perp(x, \mathbf{p}_T^2)$  [35], named as the Boer–Mulders function later, as one of the eight leading-twist 3dPDFs or TMD distribution functions contained in [36, 37]

$$\begin{aligned} \Phi = \frac{1}{2} \left\{ f_1 \not{n}_+ - f_{1T}^\perp \frac{\varepsilon_T^{ij} p_{Ti} S_{Tj}}{M} \not{n}_+ + h_{1T} \frac{[\not{S}_T, \not{n}_+]}{2} \gamma_5 \right. \\ + \left( S_{Lg_{1L}} + \frac{\mathbf{p}_T \cdot \mathbf{S}_T}{M} g_{1T} \right) \gamma_5 \not{n}_+ \\ + \left( S_{Lh_{1L}^\perp} + \frac{\mathbf{p}_T \cdot \mathbf{S}_T}{M} h_{1T}^\perp \right) \frac{[\not{p}_T, \not{n}_+]}{2M} \gamma_5 \\ \left. + ih_1^\perp \frac{[\not{p}_T, \not{n}_+]}{2M} \right\}, \end{aligned} \quad (1)$$

where  $\Phi$  is the quark-quark correlation matrix, defined as

$$\Phi_{ij}(p, P, S) = \int \frac{d^4 \xi}{(2\pi)^4} e^{ip \cdot \xi} \langle PS | \bar{\psi}_j(0) \not{W}[0, \xi] \psi_i(\xi) | PS \rangle. \quad (2)$$

The sizable  $\cos 2\phi$  azimuthal asymmetry can arise from a product of two Boer–Mulders functions of two incoming hadrons by establishing a preferred transverse momentum direction from the spin–transverse momentum correlation. This effect is called the Boer–Mulders effect [35]. Many theoretical and phenomenological studies are carried out along this direction [38–56].

The Boer–Mulders function  $h_1^\perp$ , as well as the Sivers function  $f_{1T}^\perp$ , is a naively time-reversal odd ( $T$ -odd) distribution function, characterizing the correlation between quark transversal momentum and quark transversal spin. Therefore, it was thought to be forbidden for a long time because of the time-reversal invariance property of QCD [57]. However the model calculations taken by Brodsky, Hwang and Schmidt indicated that these non-vanished naively  $T$ -odd distribution functions,  $h_1^\perp$  and  $f_{1T}^\perp$  can arise from the final or initial state interaction between the struck quark and the target remnant in the SIDIS and Drell–Yan processes at leading-twist level [58, 59]. In general, the path-order Wilson line, which arises from the requirement of a full QCD gauge invariant definition of 3dPDFs or TMD distribution functions, provides non-trivial phases and leads to non-vanished  $T$ -odd distribution functions [60–65]. Due to the present of the Wilson line, opposite sign of Boer–Mulders function or Sivers function in SIDIS and Drell–Yan processes is expected [65–67]

$$h_1^\perp(x, \mathbf{p}_T^2)|_{\text{SIDIS}} = -h_1^\perp(x, \mathbf{p}_T^2)|_{\text{DY}}, \quad (3)$$

$$f_{1T}^\perp(x, \mathbf{p}_T^2)|_{\text{SIDIS}} = -f_{1T}^\perp(x, \mathbf{p}_T^2)|_{\text{DY}}. \quad (4)$$

This relation still awaits for experimental confirmation. For hadron productions in hadron–hadron collisions, the situation is more involved, since colored objects exist in both the initial and the final states. The multiple final or initial state interactions will generate process-dependent 3dPDFs or TMDs which may be different from those in SIDIS or Drell–Yan process [68–71]. This is also viewed as the breakdown of the generalized 3dPDF or TMD factorization in the inclusive hadro-production of hadrons [72].

The angular differential cross section for unpolarized Drell–Yan process has the general form:

$$\begin{aligned} \frac{1}{\sigma} \frac{d\sigma}{d\Omega} = \frac{3}{4\pi} \frac{1}{\lambda + 3} \left( 1 + \lambda \cos^2 \theta + \mu \sin 2\theta \cos \phi \right. \\ \left. + \frac{\nu}{2} \sin^2 \theta \cos 2\phi \right), \end{aligned} \quad (5)$$

where  $\Omega$  is the solid angle and  $\lambda$ ,  $\mu$ , and  $\nu$  are angular distribution coefficients. For azimuthal symmetrical scattering,

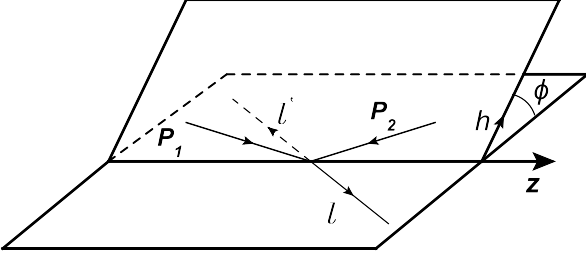


Fig. 1 The Collins–Soper frame.

the coefficients  $\mu = \nu = 0$ . The polar and azimuthal angular  $\theta$  and  $\phi$  are defined in the Collins–Soper (CS) frame [73], as shown in Fig. 1. It is the center of mass of the lepton pair with the  $z$  axis defined as the bisector of two incoming hadrons. The polar angular  $\theta$  is defined as the angular of the positive lepton with respect to the  $z$  axis direction, and the azimuthal angular  $\phi$  is defined as the angular of the lepton plane with respect to the proton plane. In this frame the Lam–Tung relation is insensitive to the higher fixed-order perturbative QCD [74] or the QCD resummation [75–77].

Taking into account the Boer–Mulders distribution, we can express the unpolarized Drell–Yan cross section as

$$\frac{d\sigma}{d\Omega dx_1 dx_2 d^2\mathbf{q}_T} = \frac{\alpha_{\text{em}}^2}{12Q^2} \sum_a e_a^2 \left\{ (1 + \cos^2 \theta) \mathcal{F}[f_{1a} \bar{f}_{1a}] + \sin^2 \theta \cos 2\phi \mathcal{F} \left[ \frac{2\hat{\mathbf{h}} \cdot \mathbf{p}_T \hat{\mathbf{h}} \cdot \mathbf{k}_T - \mathbf{p}_T \cdot \mathbf{k}_T}{m_N^2} h_{1a}^\perp \bar{h}_{1a}^\perp \right] \right\}, \quad (6)$$

where  $\hat{\mathbf{h}} \equiv \mathbf{q}_T / |\mathbf{q}_T|$  is the direction of the transversal momentum transfer,  $\mathbf{p}_T$  and  $\mathbf{k}_T$  are the transversal momentum of quarks in the nucleons,  $m_N$  is the mass of a nucleon,  $\alpha_{\text{em}}$  is the electromagnetic fine structure constant and  $e_a$  is the charge of the quark with the subscript  $a$  showing the flavor. The structure function notation in the equation is defined as

$$\mathcal{F}[\dots] = \int d^2\mathbf{p}_T d^2\mathbf{k}_T \delta^2(\mathbf{p}_T + \mathbf{k}_T - \mathbf{q}_T) [\dots]. \quad (7)$$

Then the  $\cos 2\phi$  azimuthal asymmetry can be expressed as

$$v = \frac{2 \frac{1}{Q^2} \sum_a e_a^2 \mathcal{F} \left[ \frac{2\hat{\mathbf{h}} \cdot \mathbf{p}_T \hat{\mathbf{h}} \cdot \mathbf{k}_T - \mathbf{p}_T \cdot \mathbf{k}_T}{m_N^2} h_{1a}^\perp \bar{h}_{1a}^\perp \right]}{\frac{1}{Q^2} \sum_a e_a^2 \mathcal{F}[f_{1a} \bar{f}_{1a}]}. \quad (8)$$

If we take both  $\gamma^*$  and  $Z$  boson into account, the cross section is expressed as [35]

$$\frac{d\sigma}{d\Omega dx_1 dx_2 d^2\mathbf{q}_T} = \frac{\alpha_{\text{em}}^2}{3Q^2} \sum_a \left\{ K_1(\theta) \mathcal{F}[f_{1a} \bar{f}_{1a}] + [K_3(\theta) \cos 2\phi + K_4(\theta) \sin 2\phi] \times \mathcal{F} \left[ (2\hat{\mathbf{h}} \cdot \mathbf{p}_T \hat{\mathbf{h}} \cdot \mathbf{k}_T - \mathbf{p}_T \cdot \mathbf{k}_T) \frac{h_{1a}^\perp \bar{h}_{1a}^\perp}{m_N^2} \right] \right\}. \quad (9)$$

The coefficients  $K_1, K_2, K_3, K_4$  are expressed as

$$K_1(\theta) = \frac{1}{4} (1 + \cos^2 \theta) [e_a^2 + 2g_\ell^V e_a g_a^V \chi_1 + c_1^\ell c_1^a \chi_2] + \frac{\cos \theta}{2} [2g_\ell^A e_a g_a^A \chi_1 + c_3^\ell c_3^a \chi_2], \quad (10)$$

$$K_2(\theta) = \frac{1}{4} (1 + \cos^2 \theta) [2g_\ell^V e_a g_a^A \chi_1 + c_1^\ell c_3^a \chi_2] + \frac{\cos \theta}{2} [2g_\ell^A e_a g_a^V \chi_1 + c_3^\ell c_1^a \chi_2], \quad (11)$$

$$K_3(\theta) = \frac{1}{4} \sin^2 \theta [e_a^2 + 2g_\ell^V e_a g_a^V \chi_1 + c_1^\ell c_2^a \chi_2], \quad (12)$$

$$K_4(\theta) = \frac{1}{4} \sin^2 \theta [2g_\ell^V e_a g_a^A \chi_3], \quad (13)$$

where the combinations of the coupling constants are

$$c_1^j = (g_j^{V^2} + g_j^{A^2}), \quad c_2^j = (g_j^{V^2} - g_j^{A^2}), \quad (14)$$

$$c_3^j = 2g_j^V g_j^A,$$

and the  $Z$  boson propagator factors are expressed as

$$\chi_1 = \frac{1}{\sin^2(2\theta_W)} \frac{Q^2(Q^2 - m_Z^2)}{(Q^2 - m_Z^2)^2 + \Gamma_Z^2 m_Z^2}, \quad (15)$$

$$\chi_2 = \frac{1}{\sin^2(2\theta_W)} \frac{Q^2}{Q^2 - m_Z^2} \chi_1, \quad (16)$$

$$\chi_3 = -\frac{\Gamma_Z m_Z}{Q^2 - m_Z^2} \chi_1, \quad (17)$$

where  $\theta_W$  is the Weinberg angle. Then the  $\cos 2\phi$  azimuthal asymmetry is

$$v = \frac{2 \sum_a \frac{e_a^2 + 2g_\ell^V e_a g_a^V \chi_1 + c_1^\ell c_1^a \chi_2}{Q^2} \mathcal{F} \left[ \frac{2\hat{\mathbf{h}} \cdot \mathbf{p}_T \hat{\mathbf{h}} \cdot \mathbf{k}_T - \mathbf{p}_T \cdot \mathbf{k}_T}{m_N^2} h_{1a}^\perp \bar{h}_{1a}^\perp \right]}{\sum_a \frac{e_a^2 + 2g_\ell^V e_a g_a^V \chi_1 + c_1^\ell c_1^a \chi_2}{Q^2} \mathcal{F}[f_{1a} \bar{f}_{1a}]}. \quad (18)$$

Another azimuthal dependent term is the  $\sin 2\phi$  term in Eq. (9). However the  $\sin 2\phi$  term is  $1/Q^2$  suppressed. This suppression can be found from (13) and (17).

For  $pd$  dilepton production processes, we assume the isospin relation. The distribution functions of  $u$  or  $\bar{u}$  quark in proton is the same as those of  $d$  or  $\bar{d}$  quark in neutron, and the distribution functions of  $d$  or  $\bar{d}$  quark in proton is the same as those of  $u$  or  $\bar{u}$  quark in neutron. We can also neglect the nuclear effect of deuteron, since it is a weakly bound state of a proton and a neutron. Therefore, for  $pd$  processes, we need to replace the 3dPDFs or TMDs of the target proton in Eq. (8)(18) as

$$f_u \rightarrow \frac{1}{2}(f_u + f_d), \quad (19)$$

with  $f$  representing  $f_1$  or  $h_1^\perp$  and similar for  $d, \bar{u}$  and  $\bar{d}$  quarks. Then we can get the  $\cos 2\phi$  azimuthal asymmetry coefficient  $v$  for  $pd$  dilepton production in Drell–Yan continuum region and around the  $Z$  pole.

### 3 The $\sin(2\phi - \phi_S)$ , $\sin(2\phi + \phi_S)$ and $\sin 2\phi$ azimuthal asymmetries of single polarized $pp$ and $pd$ processes

Large SSAs observed experimentally [15–27] cannot be interpreted by the standard perturbative QCD based on collinear factorization to leading twist. As a challenging issue in hadron structure and QCD spin physics, many theoretical studies were proposed to explain origin of such asymmetries [78–83]. In the 3PDF or TMD framework, the non-vanished naively  $T$ -odd Sivers function  $f_{1T}^\perp$  in Eq.(1), which characterizes the correlation between quark transversal momentum and hadron transversal spin, was applied to explain the SSAs observed in the process  $pp^\uparrow \rightarrow \pi X$  [79–82]. SSAs contributed by this Sivers effect in SIDIS processes with one nucleon transversally polarized have been measured by several experiments in recent years [21–23, 26, 27, 84–86]. The data on the Sivers SSAs have been utilized by different groups to extract the Sivers function of the proton on the basis of the 3PDF or TMD factorization [67, 87–93].

For a fixed-target experiment, it is convenient to polarized the target to allow the SSAs measurements. Five leading twist 3PDFs or TMDs in Eq. (1),  $f_{1T}^\perp$ ,  $h_1^\perp$ ,  $h_{1T}^\perp$ ,  $g_{1T}$  and  $h_{1L}^\perp$ , vanish upon integrating over the transversal momentum  $\mathbf{k}_T$ . The two naively  $T$ -odd distribution function  $f_{1T}^\perp$ , the Sivers function, and  $h_1^\perp$ , the Boer–Mulders function are account for the SSAs in various processes. Four leading twist 3PDFs or TMDs,  $h_{1T}$ ,  $h_1^\perp$ ,  $h_{1T}^\perp$  and  $h_{1L}^\perp$ , are chirally odd, so they describe densities of the probed quarks with helicity flipped. The  $h_{1T}$  and  $h_{1T}^\perp$  have the relation with the  $h_1$  that

$$h_1(x, \mathbf{k}_T^2) = h_{1T}(x, \mathbf{k}_T^2) + \frac{\mathbf{k}_T^2}{2m_N^2} h_{1T}^\perp(x, \mathbf{k}_T^2). \quad (20)$$

The distribution functions  $h_1$  and  $h_1^\perp$  respectively characterize the densities of transversely polarized quarks inside a transversely polarized proton and an unpolarized proton. The distribution functions  $h_{1T}^\perp$  and  $h_{1L}^\perp$ , arising from the double spin correlations in the parton distribution functions, respectively describe the densities of transversely polarized quarks in a transversely orthogonally polarized proton and longitudinally polarized proton.

The chiral-odd 3PDFs or TMDs are rather difficult to be probed in high energy scattering experiments, because they only manifest their effects by combining with another chiral-odd function, Collins fragmentation function in SIDIS or another chiral-odd distribution function in Drell–Yan. Some efforts have been made to extract the transversity from SIDIS data [94, 95] and to extract the Boer–Mulders function from SIDIS and Drell–Yan data [47, 49, 50, 96]. There are some extensive model calculations of  $h_{1T}^\perp$  and  $h_{1L}^\perp$  [83, 97–107].

If the transverse momentum of the dilepton in the Drell–Yan process  $\mathbf{q}_T$  is measured, we can apply the 3PDF or TMD factorization [62, 67, 92, 93], which is valid in  $q_T^2 \ll$

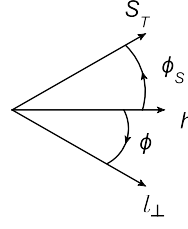


Fig. 2 The definition of azimuthal angles.

$Q^2$  region. Then the leading order of the differential cross section can be expressed as [35, 108]

$$\begin{aligned} \frac{d\sigma}{d\Omega dx_1 dx_2 d^2\mathbf{q}_T} = & \frac{\alpha_{em}}{3Q^2} \sum_a e_a^2 \left\{ \frac{1}{4} (1 + \cos^2 \theta) \mathcal{F}[f_{1a} \bar{f}_{1a}] \right. \\ & + S_L \frac{\sin^2 \theta}{4} \sin 2\phi \mathcal{F} \left[ \frac{2(\hat{\mathbf{h}} \cdot \mathbf{p}_T)(\hat{\mathbf{h}} \cdot \mathbf{k}_T) - \mathbf{p}_T \cdot \mathbf{k}_T}{m_N^2} h_{1La}^\perp \bar{h}_{1a}^\perp \right] \\ & + |\mathbf{S}_T| \frac{\sin^2 \theta}{4} \left[ \sin(2\phi + \phi_S) \mathcal{F} \left[ (2(\hat{\mathbf{h}} \cdot \mathbf{p}_T)(2(\hat{\mathbf{h}} \cdot \mathbf{p}_T)(\hat{\mathbf{h}} \cdot \mathbf{k}_T) \right. \right. \\ & \quad \left. \left. - \mathbf{p}_T \cdot \mathbf{k}_T) - \mathbf{p}_T^2 (\hat{\mathbf{h}} \cdot \mathbf{k}_T) \right) \frac{h_{1Ta}^\perp \bar{h}_{1a}^\perp}{2m_N^3} \right] \right. \\ & \left. + \sin(2\phi - \phi_S) \mathcal{F} \left[ \frac{\hat{\mathbf{h}} \cdot \mathbf{p}_T}{m_N} h_{1a} \bar{h}_{1a}^\perp \right] \right\} + \dots \end{aligned} \quad (21)$$

where the structure function notation is defined as Eq. (7), and the azimuthal angles  $\phi$  and  $\phi_S$  are defined as shown in Fig. 2. Therefore, one can define the following azimuthal asymmetries:

$$A_{TU}^{\sin(2\phi - \phi_S)} = \frac{\frac{1}{Q^2} \sum_a e_a^2 \mathcal{F} \left[ \frac{\hat{\mathbf{h}} \cdot \mathbf{p}_T}{m_N} h_{1a} \bar{h}_{1a}^\perp \right]}{\frac{1}{Q^2} \sum_a e_a^2 \mathcal{F}[f_{1a} \bar{f}_{1a}]}, \quad (22)$$

$$A_{TU}^{\sin(2\phi + \phi_S)} = \frac{\frac{1}{Q^2} \sum_a e_a^2 \mathcal{F} \left[ \frac{2(\hat{\mathbf{h}} \cdot \mathbf{p}_T)(2(\hat{\mathbf{h}} \cdot \mathbf{p}_T)(\hat{\mathbf{h}} \cdot \mathbf{k}_T) - \mathbf{p}_T \cdot \mathbf{k}_T) - \mathbf{p}_T^2 (\hat{\mathbf{h}} \cdot \mathbf{k}_T)}{2m_N^3} h_{1La}^\perp \bar{h}_{1a}^\perp \right]}{\frac{1}{Q^2} \sum_a e_a^2 \mathcal{F}[f_{1a} \bar{f}_{1a}]}, \quad (23)$$

$$A_{LU}^{\sin 2\phi} = \frac{\frac{1}{Q^2} \sum_a e_a^2 \mathcal{F} \left[ \frac{2(\hat{\mathbf{h}} \cdot \mathbf{p}_T)(\hat{\mathbf{h}} \cdot \mathbf{k}_T) - \mathbf{p}_T \cdot \mathbf{k}_T}{m_N^2} h_{1La}^\perp \bar{h}_{1a}^\perp \right]}{\frac{1}{Q^2} \sum_a e_a^2 \mathcal{F}[f_{1a} \bar{f}_{1a}]}. \quad (24)$$

If we take both  $\gamma^*$  and  $Z$  boson into account, the cross section is expressed as [35]

$$\begin{aligned} \frac{d\sigma}{d\Omega dx_1 dx_2 d^2\mathbf{q}_T} &= \frac{\alpha_{\text{em}}}{3Q^2} \sum_a \left\{ K_1(\theta) \mathcal{F}[f_{1a}\bar{f}_{1a}] \right. \\ &+ S_L [K_3(\theta) \sin 2\phi + K_4(\theta) \cos 2\phi] \\ &\times \mathcal{F} \left[ \frac{2(\hat{\mathbf{h}} \cdot \mathbf{p}_T)(\hat{\mathbf{h}} \cdot \mathbf{k}_T) - \mathbf{p}_T \cdot \mathbf{k}_T}{m_N^2} h_{1La}^\perp \bar{h}_{1a}^\perp \right] \\ &+ |\mathbf{S}_T| \left[ [K_3(\theta) \sin(2\phi + \phi_S) + K_4(\theta) \cos(2\phi + \phi_S)] \right. \\ &\times \mathcal{F} \left[ (2(\hat{\mathbf{h}} \cdot \mathbf{p}_T)(2(\hat{\mathbf{h}} \cdot \mathbf{p}_T)(\hat{\mathbf{h}} \cdot \mathbf{k}_T) \right. \\ &\quad \left. \left. - \mathbf{p}_T \cdot \mathbf{k}_T) - \mathbf{p}_T^2 (\hat{\mathbf{h}} \cdot \mathbf{k}_T) \right) \frac{h_{1Ta}^\perp \bar{h}_{1a}^\perp}{2m_N^3} \right] \\ &+ [K_3(\theta) \sin(2\phi - \phi_S) + K_4(\theta) \cos(2\phi - \phi_S)] \\ &\left. \times \mathcal{F} \left[ \frac{\hat{\mathbf{h}} \cdot \mathbf{p}_T}{m_N} h_{1a} \bar{h}_{1a}^\perp \right] \right] + \dots \left. \right\}, \end{aligned} \quad (25)$$

where the coefficients  $K_1(\theta)$ ,  $K_3(\theta)$  and  $K_4(\theta)$  are defined in (10)–(13). Then the azimuthal asymmetries defined in (22)–(24) are expressed with  $Z$  taken into account as

$$A_{TU}^{\sin(2\phi - \phi_S)} = \frac{2 \sum_a K_3(\theta) \mathcal{F} \left[ \frac{\hat{\mathbf{h}} \cdot \mathbf{p}_T}{m_N} h_{1a} \bar{h}_{1a}^\perp \right]}{\sum_a K_1(\theta) \mathcal{F}[f_{1a}\bar{f}_{1a}]}, \quad (26)$$

$$A_{TU}^{\sin(2\phi + \phi_S)} = \quad (27)$$

$$\begin{aligned} &\frac{2 \sum_a K_3(\theta) \mathcal{F} \left[ \frac{2(\hat{\mathbf{h}} \cdot \mathbf{p}_T)(2(\hat{\mathbf{h}} \cdot \mathbf{p}_T)(\hat{\mathbf{h}} \cdot \mathbf{k}_T) - \mathbf{p}_T \cdot \mathbf{k}_T) - \mathbf{p}_T^2 (\hat{\mathbf{h}} \cdot \mathbf{k}_T)}{2m_N^3} h_{1Ta}^\perp \bar{h}_{1a}^\perp \right]}{\sum_a K_1(\theta) \mathcal{F}[f_{1a}\bar{f}_{1a}]}, \\ A_{LU}^{\sin 2\phi} &= \frac{2 \sum_a K_3(\theta) \mathcal{F} \left[ \frac{2(\hat{\mathbf{h}} \cdot \mathbf{p}_T)(\hat{\mathbf{h}} \cdot \mathbf{k}_T) - \mathbf{p}_T \cdot \mathbf{k}_T}{m_N^2} h_{1La}^\perp \bar{h}_{1a}^\perp \right]}{\sum_a K_1(\theta) \mathcal{F}[f_{1a}\bar{f}_{1a}]}. \end{aligned} \quad (28)$$

The  $\cos 2\phi$ ,  $\cos(2\phi - \phi_S)$  and  $\cos(2\phi + \phi_S)$  azimuthal dependent terms are  $1/Q^2$  suppressed. This suppression can be found from (13) and (17).

For  $pd$  dilepton production processes with the deuteron longitudinally or transversely polarized, we assume the isospin symmetry and neglect the nuclear effect as we do for unpolarized  $pd$  processes. Therefore, we can get the  $\sin(2\phi - \phi_S)$ ,  $\sin(2\phi + \phi_S)$  and  $\sin 2\phi$  azimuthal asymmetries of  $pd$  dilepton production processes in Drell–Yan continuum region and around the  $Z$  pole by replacing the distribution functions of the target via (19).

#### 4 Numerical results

In this section, we calculate the azimuthal asymmetries of the  $pp$  and  $pd$  dilepton production processes with the proton or deuteron target unpolarized and longitudinally or transversally polarized in Drell–Yan continuum region and  $Z$  resonance region respectively. We present a numerical estimation of these azimuthal asymmetries for measurement at a

fixed-target experiment using the LHC beams proposed by Brodsky, Fleuret, Hadjidakis and Lansberg [1]. With the 7 TeV proton beams, the center-of-mass frame energy  $\sqrt{s} = 115$  GeV for two nucleons.

The cross section of Drell–Yan process can also be expressed depending on  $y$  and  $Q^2$  instead of  $x_1$  and  $x_2$  with just a Jacobian multiplied as

$$\frac{d\sigma}{dy dQ^2 d^2\mathbf{q}_T d\Omega} = \frac{1}{s} \frac{d\sigma}{dx_1 dx_2 d^2\mathbf{q}_T d\Omega}. \quad (29)$$

At the region  $\mathbf{q}_T^2 \ll Q^2$ , we have the following relation:

$$x_1 = \frac{Q}{\sqrt{s}} e^y, \quad x_2 = \frac{Q}{\sqrt{s}} e^{-y}. \quad (30)$$

The  $x_1$  and  $x_2$  can also be expressed with  $x_F$  and  $Q^2$

$$\begin{aligned} x_1 &= \frac{1}{2} \left( x_F + \sqrt{x_F^2 + 4 \frac{Q^2}{s}} \right), \\ x_2 &= \frac{1}{2} \left( -x_F + \sqrt{x_F^2 + 4 \frac{Q^2}{s}} \right), \end{aligned} \quad (31)$$

and

$$x_F = x_1 - x_2. \quad (32)$$

$x_1$  is the momentum fraction of the parton in the beam proton, and  $x_2$  is that of the parton in the target nucleon. For the single polarized processes,  $x_2$  is the momentum fraction of the parton in the polarized target nucleon, sometimes labeled as  $x^\uparrow$  in the literature. To calculate the azimuthal asymmetries depending on  $Q$ ,  $x_F$  or  $q_T$ , we need to integrate over the other variables in the numerator and the dominator of the expression of the asymmetries respectively. The rapidity is cut in  $[-4.8, 1]$  which is the easiest region to carry on measurements as discussed in [1], and this is where the momentum fraction of the parton inside the polarized nucleons is the largest.

In our calculation, we adopt the Boer–Mulders function  $h_1^\perp$  extracted from the unpolarized  $pd$  and  $pp$  Drell–Yan data [13, 14, 47, 50]. The parametrization of  $h_1^\perp$  for both valence and sea quarks has the form:

$$h_{1q}^\perp(x, k_T^2) = H_q x^{c^q} (1-x)^b f_{1q}(x) \frac{1}{\pi k_{\text{bm}}^2} \exp\left(\frac{-\mathbf{k}_T^2}{k_{\text{bm}}^2}\right), \quad (33)$$

where the subscript "bm" stands for the Boer–Mulders functions, and  $q = u, d, \bar{u}$  and  $\bar{d}$ . The possible range of the parameters  $H_q$  allowed by the positivity bound [109] can be described by a coefficient  $\omega$  which balance the contributions of quark and antiquark.  $H_q \rightarrow \omega H_q$  for  $q = u, d$  and  $H_q \rightarrow \omega^{-1} H_q$  for  $q = \bar{u}, \bar{d}$  will not change the calculated  $\cos 2\phi$  asymmetry in the unpolarized  $pp$  and  $pd$  Drell–Yan data. The range of  $\omega$  is  $0.48 < \omega < 2.1$ , and we choose the

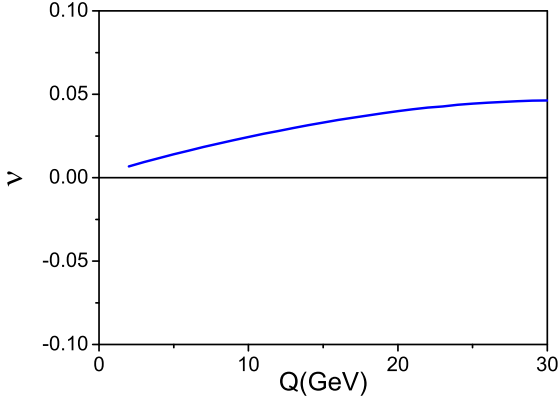


**Fig. 3** The  $\cos 2\phi$  azimuthal asymmetry depending on  $Q$  of unpolarized  $pp$  Drell–Yan process with both  $\gamma^*$  and  $Z$  taken into account and allowed rapidity integrated in the cut  $[-4.8, 1]$ . The same cut of rapidity is chosen in Figs.7,11-16.

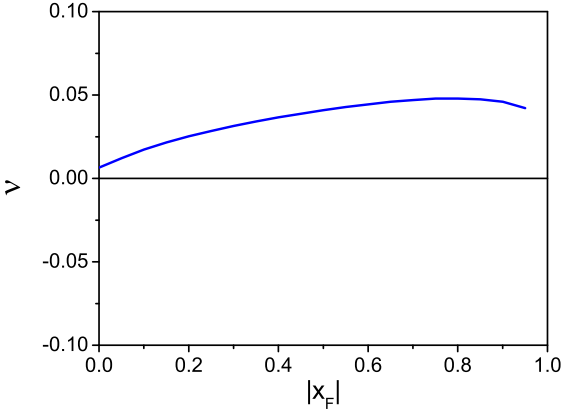


**Fig. 4** The  $\cos 2\phi$  azimuthal asymmetry depending on  $x_F$  of unpolarized  $pp$  Drell–Yan process at  $Q = 2$  GeV.

case  $\omega = 1$ , which corresponds to the central values of  $H_q$ , in our calculation.

In Figs. 3 and 7, we show the  $\cos 2\phi$  azimuthal asymmetry depending on  $Q$  from 2 GeV to 30 GeV of the unpolarized  $pp$  and  $pd$  Drell–Yan process at AFTER including  $Z$  taken into account. Figs. 4, 5, 8 and 9 respectively show the  $\cos 2\phi$  azimuthal asymmetry depending on  $x_F$  of the unpolarized  $pp$  and  $pd$  processes with  $Q = 2$  GeV and  $Q = 5$  GeV as for low and mid  $Q$  Drell–Yan regions at AFTER. Figs. 6 and 10 respectively show this azimuthal asymmetry of  $pp$  and  $pd$  processes at the  $Z$  pole at AFTER.

To calculate the SSAs of the  $pp$  and  $pd$  dilepton production processes at AFTER, we also need the distribution functions  $h_{1T}^\perp$ ,  $h_{1L}^\perp$  and  $h_1$  besides the Boer–Mulders function  $h_1^\perp$ . In our calculation, we adopt ansatz of these  $T$ -even distribution functions calculated from the light-cone quark-diquark model. In this model, the Melosh–Wigner rotation, which is important to understand the proton spin puzzle due to the

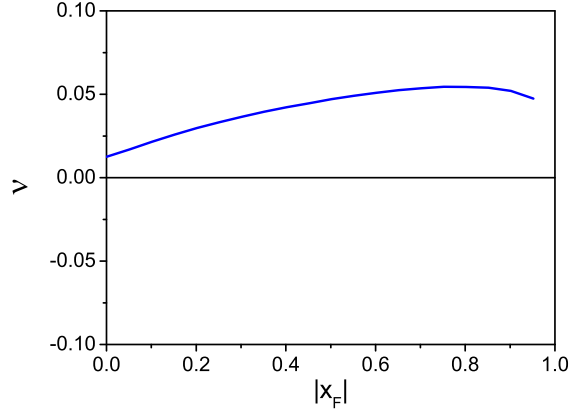


**Fig. 5** The  $\cos 2\phi$  azimuthal asymmetry depending on  $x_F$  of unpolarized  $pp$  Drell–Yan process at  $Q = 5$  GeV.

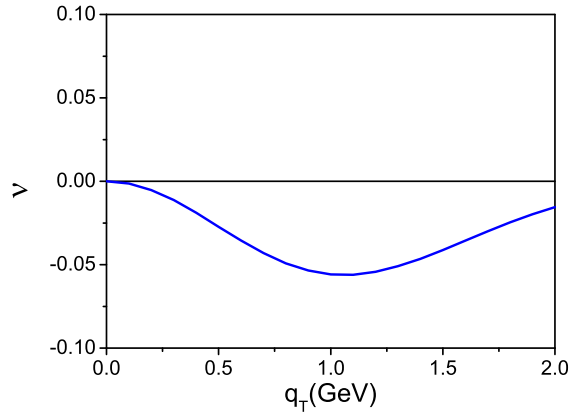


**Fig. 6** The  $\cos 2\phi$  azimuthal asymmetry depending on  $q_T$  of unpolarized  $pp$  process in  $Z$  resonance region.

relativistic effect of quark transversal motions [110–113], is taken into account. This model has been applied to calculate helicity distributions [114], transversity distributions [115, 116] and some other 3dPDFs or TMDs [100, 104, 117], and has been used to analysis related azimuthal spin asymmetries in SIDIS processes [118, 119]. The model results of these distribution functions are expressed as [100, 104, 115, 116]

$$j_{ud}^v(x, \mathbf{k}_T^2) = [f_{1u}^v(x, \mathbf{k}_T^2) - \frac{1}{2}f_{1d}^v(x, \mathbf{k}_T^2)]W_S^j(x, \mathbf{k}_T^2) - \frac{1}{6}f_{1d}^v(x, \mathbf{k}_T^2)W_V^j(x, \mathbf{k}_T^2), \quad (34)$$

$$j_d^v(x, \mathbf{k}_T^2) = -\frac{1}{3}f_{1d}^v(x, \mathbf{k}_T^2)W_V^j(x, \mathbf{k}_T^2), \quad (35)$$

where  $j = h_1, h_{1T}^\perp, h_{1L}^\perp$ , and the superscript  $v$  stands for valence quark distributions. The factors  $W_{S/V}^j(x, \mathbf{k}_T^2)$  are the Melosh–Wigner rotations for scalar or axial vector spectator-

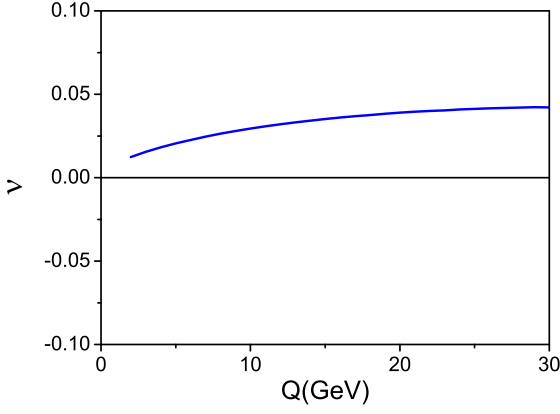


**Fig. 7** The  $\cos 2\phi$  azimuthal asymmetry depending on  $Q$  of unpolarized  $pd$  Drell-Yan process with both  $\gamma^*$  and  $Z$  taken into account.

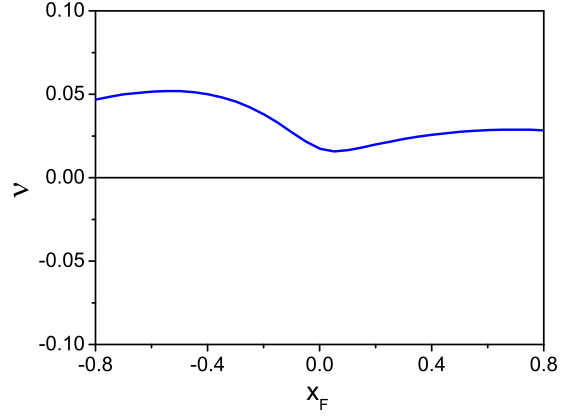


**Fig. 9** The  $\cos 2\phi$  azimuthal asymmetry depending on  $x_F$  of unpolarized  $pd$  Drell-Yan process at  $Q = 5$  GeV.

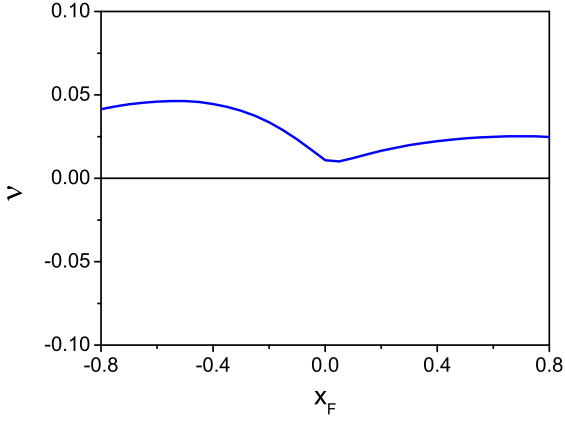


**Fig. 8** The  $\cos 2\phi$  azimuthal asymmetry depending on  $x_F$  of unpolarized  $pd$  Drell-Yan process at  $Q = 2$  GeV.

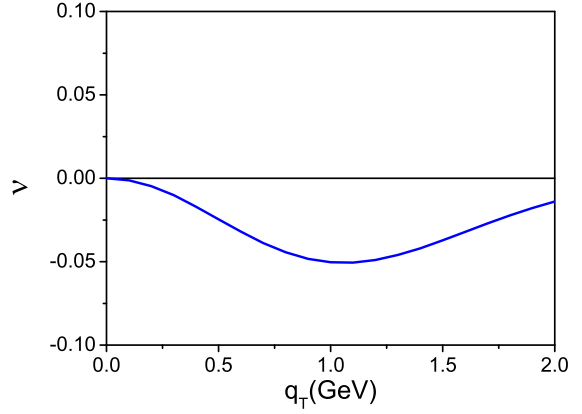


**Fig. 10** The  $\cos 2\phi$  azimuthal asymmetry depending on  $q_T$  of unpolarized  $pd$  process in  $Z$  resonance region.

diquark respectively, having the forms:

$$W_D^{h_1}(x, \mathbf{k}_T^2) = \frac{(x\mathcal{M}_D + m_q)^2}{(x\mathcal{M}_D + m_q)^2 + \mathbf{k}_T^2}, \quad (36)$$

$$W_D^{h_{1T}^\perp}(x, \mathbf{k}_T^2) = -\frac{2m_N^2}{(x\mathcal{M}_D + m_q)^2 + \mathbf{k}_T^2}, \quad (37)$$

$$W_D^{h_{1L}^\perp}(x, \mathbf{k}_T^2) = -\frac{2m_N(x\mathcal{M}_D + m_q)}{(x\mathcal{M}_D + m_q)^2 + \mathbf{k}_T^2}, \quad (38)$$

where

$$\mathcal{M}_D = \sqrt{\frac{m_q^2 + \mathbf{k}_T^2}{x} + \frac{m_D^2 + \mathbf{k}_T^2}{1-x}}. \quad (39)$$

The distribution functions  $h_1$ ,  $h_{1T}^\perp$ ,  $h_{1L}^\perp$  of sea quarks are constrained by the positivity bounds [109]:

$$\left| \bar{h}_{1q}(x, \mathbf{k}_T^2) \right| \leq \bar{f}_{1q}(x, \mathbf{k}_T^2), \quad (40)$$

$$\left| \frac{\mathbf{k}_T^2}{2m_N^2} \bar{h}_{1Tq}^\perp(x, \mathbf{k}_T^2) \right| \leq \bar{f}_{1q}(x, \mathbf{k}_T^2), \quad (41)$$

$$\left| \frac{\mathbf{k}_T}{m_N} \bar{h}_{1Lq}^\perp(x, \mathbf{k}_T^2) \right| \leq \bar{f}_{1q}(x, \mathbf{k}_T^2). \quad (42)$$

When considering the effects of these distribution functions of sea quarks contributing to the asymmetries, we can get the upper and lower limits of the azimuthal asymmetries by saturating the positivity bounds.

In Figs. 11-13, we respectively show the  $\sin(2\phi - \phi_S)$ ,  $\sin(2\phi + \phi_S)$  and  $\sin 2\phi$  azimuthal asymmetries depending on  $Q$  from 2 GeV to 30 GeV of the target proton polarized  $pp$  Drell-Yan process at AFTER including  $Z$  taken into account, and the corresponding results for deuteron target polarized  $pd$  process are shown in Figs. 14-16. These asymmetries in the far backward region, with rapidity cut  $[-4.8, -2]$ ,

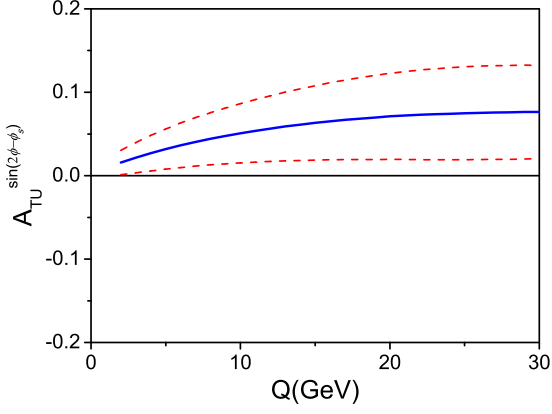


**Fig. 11** The  $\sin(2\phi - \phi_S)$  azimuthal asymmetry  $A_{TU}^{\sin(2\phi - \phi_S)}$  depending on  $Q$  of target proton polarized  $pp$  Drell-Yan process with both  $\gamma^*$  and  $Z$  taken into account. The dashed curves show the range of the asymmetry by considering the additional distributions of sea quarks constrained by the positivity bounds, corresponding to the same case as Figs. 18–40.

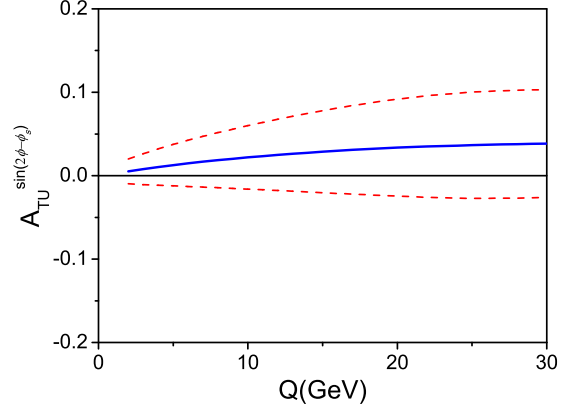


**Fig. 14** The  $\sin(2\phi - \phi_S)$  azimuthal asymmetry  $A_{TU}^{\sin(2\phi - \phi_S)}$  depending on  $Q$  of target deuteron polarized  $pd$  Drell-Yan process with both  $\gamma^*$  and  $Z$  taken into account.

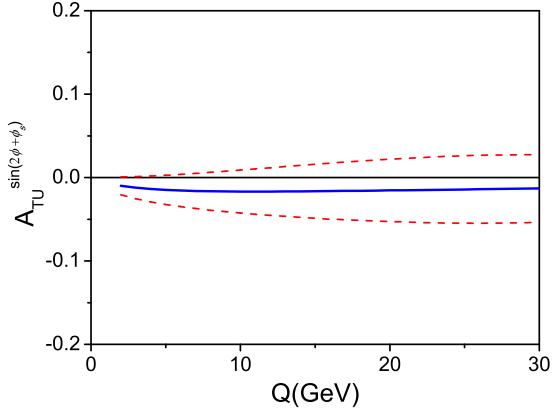


**Fig. 12** The  $\sin(2\phi + \phi_S)$  azimuthal asymmetry  $A_{TU}^{\sin(2\phi + \phi_S)}$  depending on  $Q$  of target proton polarized  $pp$  Drell-Yan process with both  $\gamma^*$  and  $Z$  taken into account.

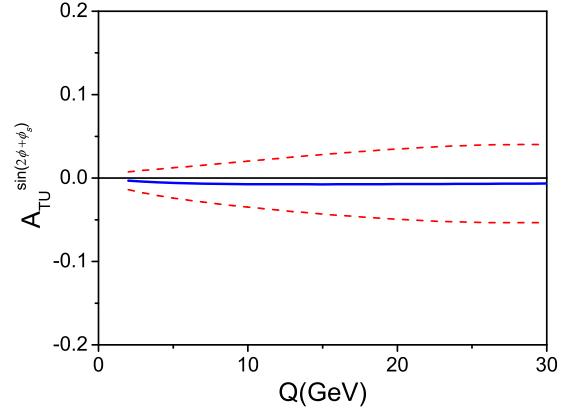


**Fig. 15** The  $\sin(2\phi + \phi_S)$  azimuthal asymmetry  $A_{TU}^{\sin(2\phi + \phi_S)}$  depending on  $Q$  of target deuteron polarized  $pd$  Drell-Yan process with both  $\gamma^*$  and  $Z$  taken into account.

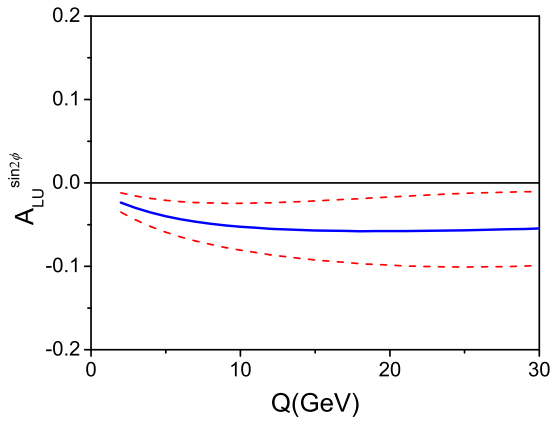


**Fig. 13** The  $\sin 2\phi$  azimuthal asymmetry  $A_{LU}^{\sin 2\phi}$  depending on  $Q$  of target proton polarized  $pp$  Drell-Yan process with both  $\gamma^*$  and  $Z$  taken into account.

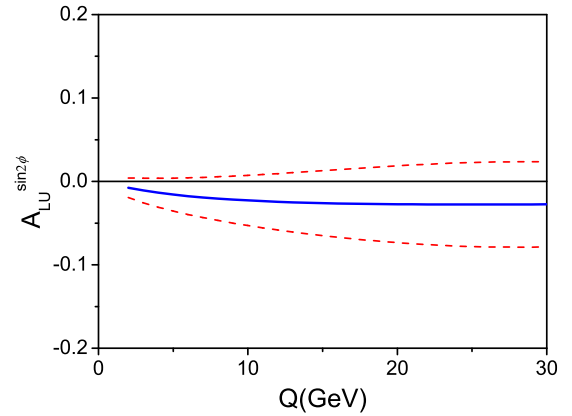


**Fig. 16** The  $\sin 2\phi$  azimuthal asymmetry  $A_{LU}^{\sin 2\phi}$  depending on  $Q$  of target deuteron polarized  $pd$  Drell-Yan process with both  $\gamma^*$  and  $Z$  taken into account.



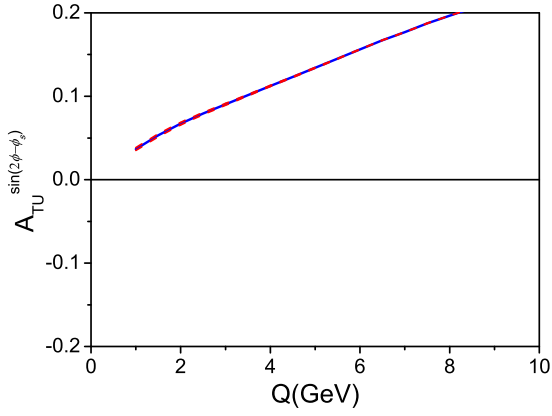


**Fig. 17** The  $\sin(2\phi - \phi_S)$  azimuthal asymmetry  $A_{TU}^{\sin(2\phi - \phi_S)}$  depending on  $Q$  of target proton polarized  $pp$  Drell-Yan process with both  $\gamma^*$  and  $Z$  taken into account and allowed rapidity integrated in the cut  $[-4.8, -2]$ . The same cut of rapidity is chosen in Figs.18-22.

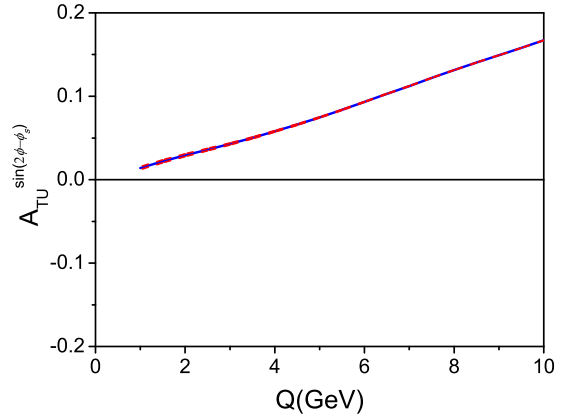


**Fig. 20** The  $\sin(2\phi - \phi_S)$  azimuthal asymmetry  $A_{TU}^{\sin(2\phi - \phi_S)}$  depending on  $Q$  of target deuteron polarized  $pd$  Drell-Yan process with both  $\gamma^*$  and  $Z$  taken into account.

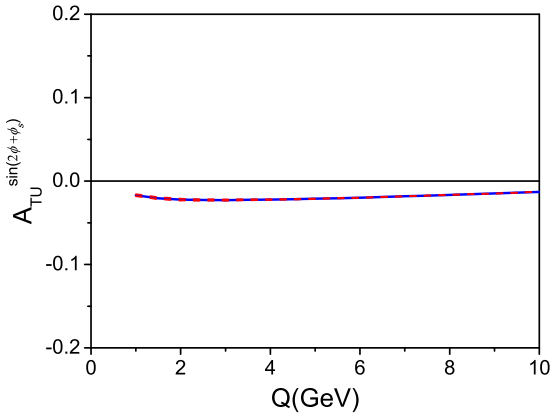


**Fig. 18** The  $\sin(2\phi + \phi_S)$  azimuthal asymmetry  $A_{TU}^{\sin(2\phi + \phi_S)}$  depending on  $Q$  of target proton polarized  $pp$  Drell-Yan process with both  $\gamma^*$  and  $Z$  taken into account.

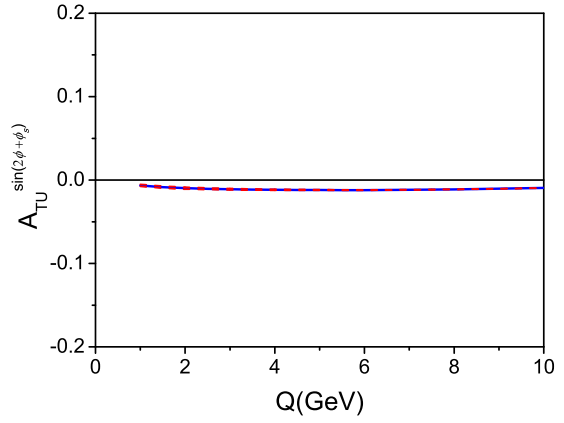


**Fig. 21** The  $\sin(2\phi + \phi_S)$  azimuthal asymmetry  $A_{TU}^{\sin(2\phi + \phi_S)}$  depending on  $Q$  of target deuteron polarized  $pd$  Drell-Yan process with both  $\gamma^*$  and  $Z$  taken into account.

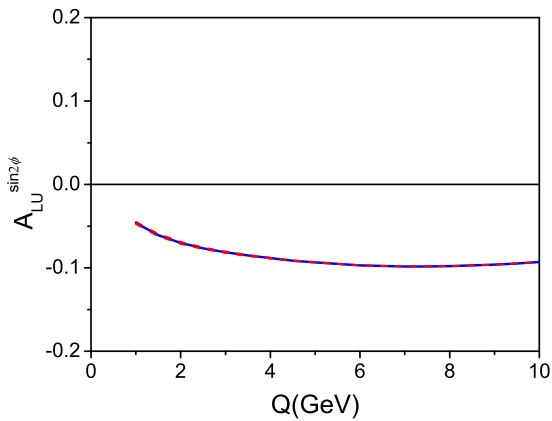


**Fig. 19** The  $\sin 2\phi$  azimuthal asymmetry  $A_{LU}^{\sin 2\phi}$  depending on  $Q$  of target proton polarized  $pp$  Drell-Yan process with both  $\gamma^*$  and  $Z$  taken into account.

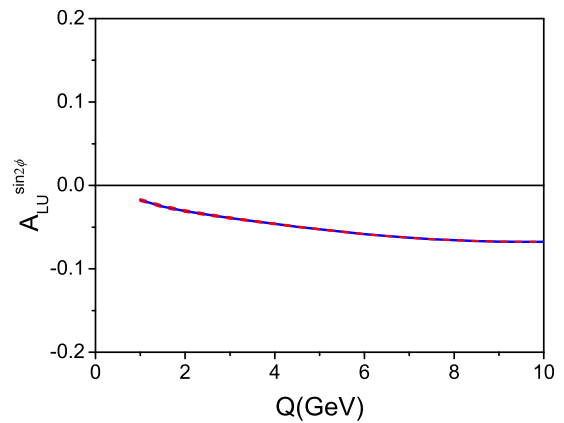


**Fig. 22** The  $\sin 2\phi$  azimuthal asymmetry  $A_{LU}^{\sin 2\phi}$  depending on  $Q$  of target deuteron polarized  $pd$  Drell-Yan process with both  $\gamma^*$  and  $Z$  taken into account.

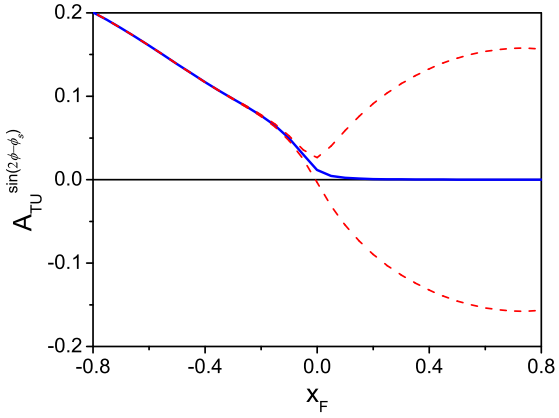


**Fig. 23** The  $\sin(2\phi - \phi_S)$  azimuthal asymmetry  $A_{TU}^{\sin(2\phi - \phi_S)}$  depending on  $x_F$  of target proton polarized  $pp$  Drell-Yan process at  $Q = 2$  GeV.

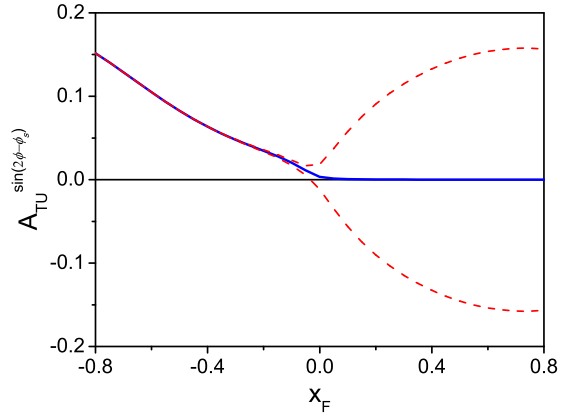


**Fig. 26** The  $\sin(2\phi - \phi_S)$  azimuthal asymmetry  $A_{TU}^{\sin(2\phi - \phi_S)}$  depending on  $x_F$  of target deuteron polarized  $pd$  Drell-Yan process at  $Q = 2$  GeV.

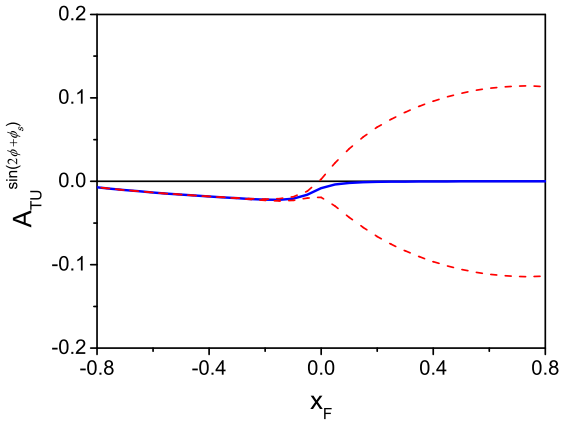


**Fig. 24** The  $\sin(2\phi + \phi_S)$  azimuthal asymmetry  $A_{TU}^{\sin(2\phi + \phi_S)}$  depending on  $x_F$  of target proton polarized  $pp$  Drell-Yan process at  $Q = 2$  GeV.

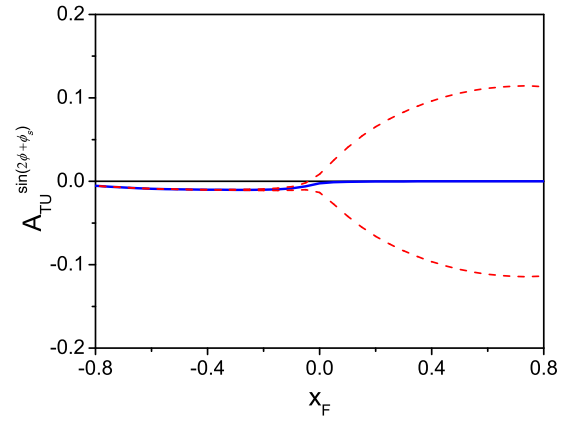


**Fig. 27** The  $\sin(2\phi + \phi_S)$  azimuthal asymmetry  $A_{TU}^{\sin(2\phi + \phi_S)}$  depending on  $x_F$  of target deuteron polarized  $pd$  Drell-Yan process at  $Q = 2$  GeV.

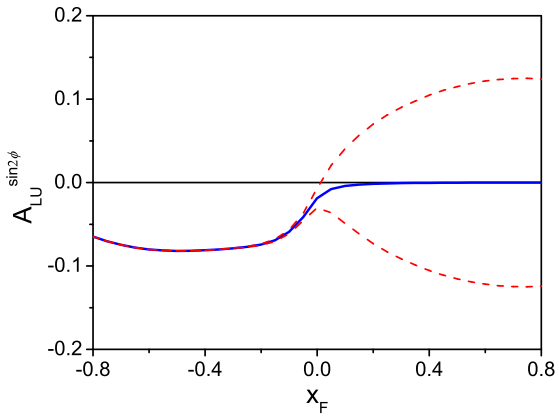


**Fig. 25** The  $\sin 2\phi$  azimuthal asymmetry  $A_{LU}^{\sin 2\phi}$  depending on  $x_F$  of target proton polarized  $pp$  Drell-Yan process at  $Q = 2$  GeV.

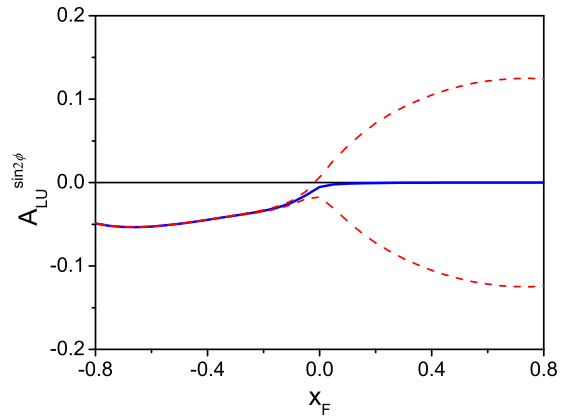


**Fig. 28** The  $\sin 2\phi$  azimuthal asymmetry  $A_{LU}^{\sin 2\phi}$  depending on  $x_F$  of target deuteron polarized  $pd$  Drell-Yan process at  $Q = 2$  GeV.

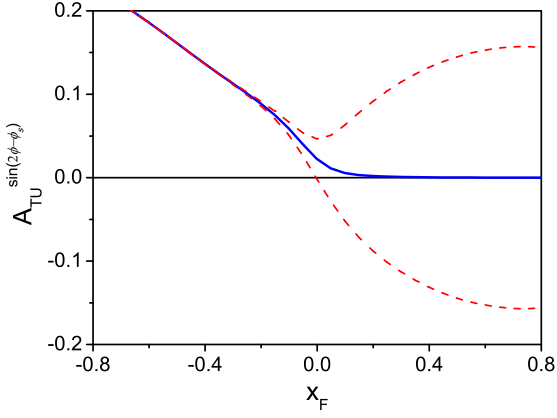


**Fig. 29** The  $\sin(2\phi - \phi_S)$  azimuthal asymmetry  $A_{TU}^{\sin(2\phi - \phi_S)}$  depending on  $x_F$  of target proton polarized  $pp$  Drell-Yan process at  $Q = 5$  GeV.

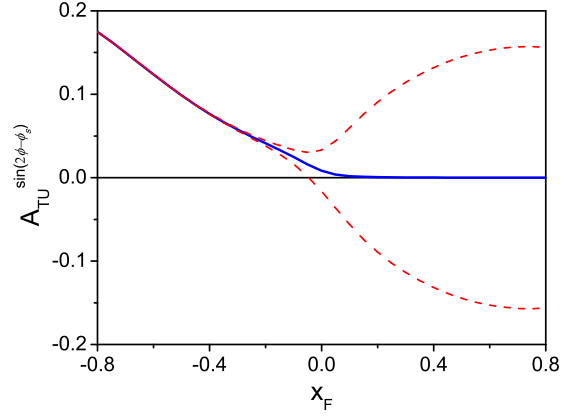


**Fig. 32** The  $\sin(2\phi - \phi_S)$  azimuthal asymmetry  $A_{TU}^{\sin(2\phi - \phi_S)}$  depending on  $x_F$  of target deuteron polarized  $pd$  Drell-Yan process at  $Q = 5$  GeV.

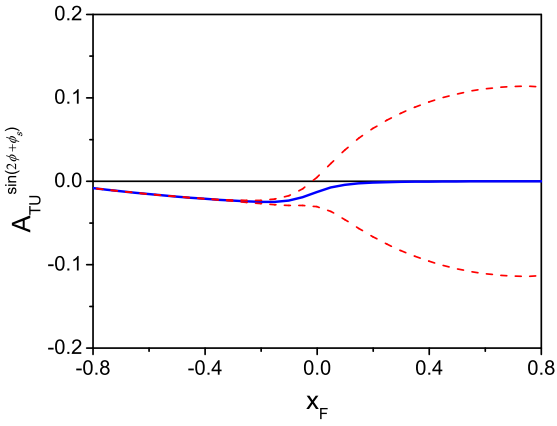


**Fig. 30** The  $\sin(2\phi + \phi_S)$  azimuthal asymmetry  $A_{TU}^{\sin(2\phi + \phi_S)}$  depending on  $x_F$  of target proton polarized  $pp$  Drell-Yan process at  $Q = 5$  GeV.

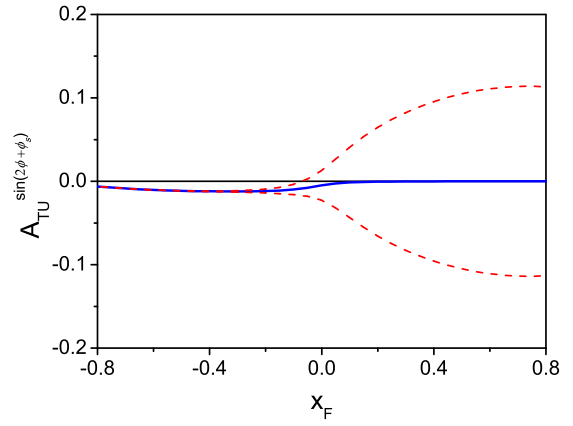


**Fig. 33** The  $\sin(2\phi + \phi_S)$  azimuthal asymmetry  $A_{TU}^{\sin(2\phi + \phi_S)}$  depending on  $x_F$  of target deuteron polarized  $pd$  Drell-Yan process at  $Q = 5$  GeV.

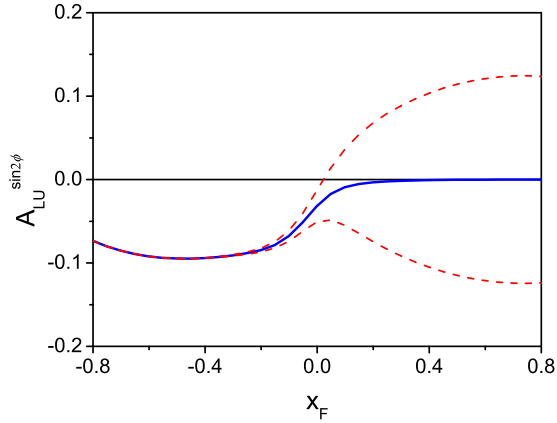


**Fig. 31** The  $\sin 2\phi$  azimuthal asymmetry  $A_{LU}^{\sin 2\phi}$  depending on  $x_F$  of target proton polarized  $pp$  Drell-Yan process at  $Q = 5$  GeV.

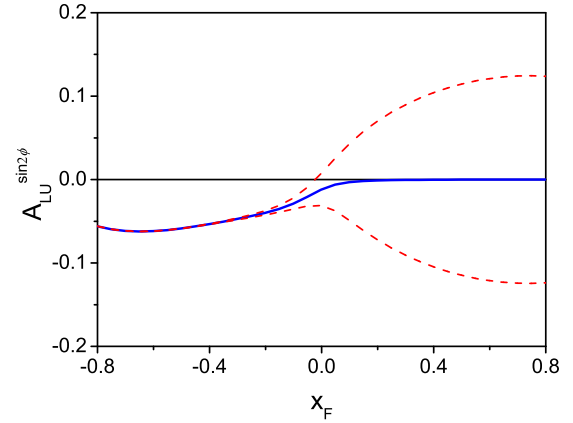


**Fig. 34** The  $\sin 2\phi$  azimuthal asymmetry  $A_{LU}^{\sin 2\phi}$  depending on  $x_F$  of target deuteron polarized  $pd$  Drell-Yan process at  $Q = 5$  GeV.

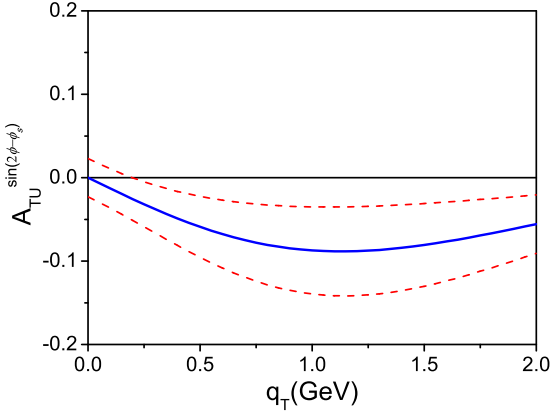


**Fig. 35** The  $\sin(2\phi - \phi_S)$  azimuthal asymmetry  $A_{TU}^{\sin(2\phi - \phi_S)}$  depending on  $q_T$  of target proton polarized  $pp$  dilepton production process at the Z pole.

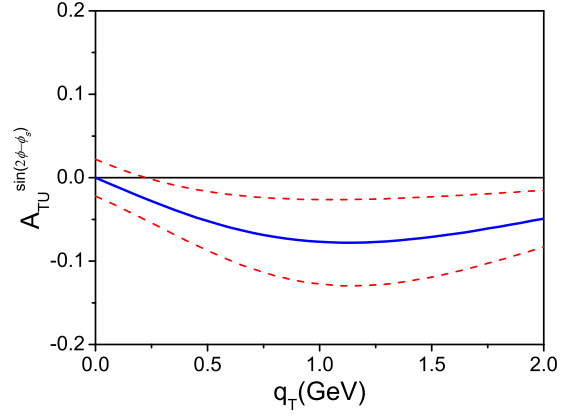


**Fig. 38** The  $\sin(2\phi - \phi_S)$  azimuthal asymmetry  $A_{TU}^{\sin(2\phi - \phi_S)}$  depending on  $q_T$  of target deuteron polarized  $pd$  dilepton production process at the Z pole.

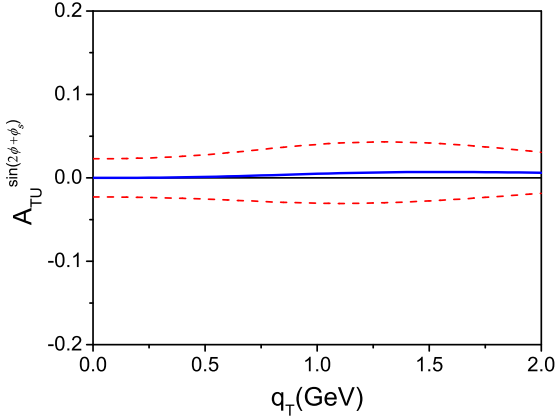


**Fig. 36** The  $\sin(2\phi + \phi_S)$  azimuthal asymmetry  $A_{TU}^{\sin(2\phi + \phi_S)}$  depending on  $q_T$  of target proton polarized  $pp$  dilepton production process at the Z pole.

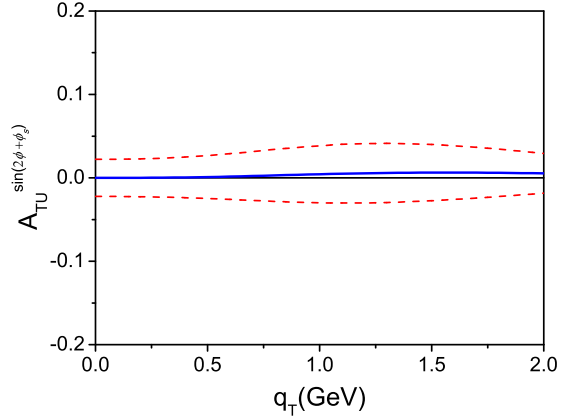


**Fig. 39** The  $\sin(2\phi + \phi_S)$  azimuthal asymmetry  $A_{TU}^{\sin(2\phi + \phi_S)}$  depending on  $q_T$  of target deuteron polarized  $pp$  dilepton production process at the Z pole.

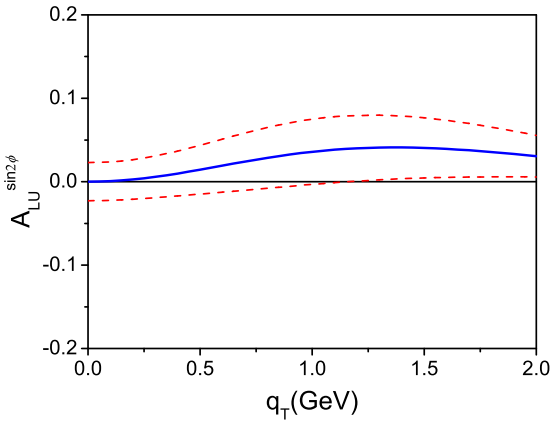


**Fig. 37** The  $\sin 2\phi$  azimuthal asymmetry  $A_{LU}^{\sin 2\phi}$  depending on  $q_T$  of target proton polarized  $pp$  dilepton production process at the Z pole.

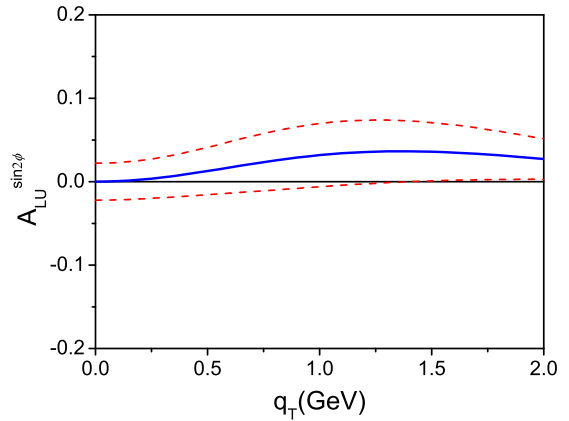


**Fig. 40** The  $\sin 2\phi$  azimuthal asymmetry  $A_{LU}^{\sin 2\phi}$  depending on  $q_T$  of target deuteron polarized  $pd$  dilepton production process at the Z pole.

are shown in Figs. 17–22, with  $Q$  running from 1 GeV to 10 GeV. In Figs. 23–34, we respectively show the  $\sin(2\phi - \phi_S)$ ,  $\sin(2\phi + \phi_S)$  and  $\sin 2\phi$  azimuthal asymmetries depending on  $x_F$  of the target proton and deuteron polarized  $pp$  and  $pd$  Drell–Yan processes at AFTER with  $Q = 2$  GeV and  $Q = 5$  GeV as for low and mid  $Q$  regions. Figs. 35–37 show the  $\sin(2\phi - \phi_S)$ ,  $\sin(2\phi + \phi_S)$  and  $\sin 2\phi$  azimuthal asymmetries of the target proton polarized  $pp$  process around the Z-pole at AFTER. The corresponding azimuthal asymmetries of  $pd$  processes with target deuteron transversally or longitudinally polarized are shown in Figs. 38–40.

## 5 Discussion and conclusions

In this paper, we calculate the  $\cos 2\phi$  azimuthal asymmetries of unpolarized  $pp$  and  $pd$  dilepton production processes in the Drell–Yan continuum region and around the Z resonance region. We also calculate the  $\sin(2\phi - \phi_S)$ ,  $\sin(2\phi + \phi_S)$  and  $\sin 2\phi$  azimuthal asymmetries of single transversally or longitudinally polarized  $pp$  and  $pd$  dilepton production processes in these regions.

Our calculations are concentrated on some issues related to the spin physics part of the AFTER project, a multi-purpose fixed-target experiment using the proton and lead-ion beams of the LHC extracted by a bent crystal, proposed by Brodsky, Fleuret, Hadjidakis and Lansberg [1]. We present an estimation of the azimuthal asymmetries for a fixed-target experiment using the LHC 7 TeV proton beams with the proton or deuteron target unpolarized and transversally or longitudinally polarized. As the target is conveniently polarized, it is an ideal ground to study the spin physics at AFTER with  $\sqrt{s} = 115$  GeV and high luminosity. It is feasible to measure these azimuthal asymmetries at AFTER. This will help us to study the three dimensional or transverse momentum dependent parton distributions (3dPDFs or TMDs), and consequently help understand and test the QCD and hadron structure at such a high laboratory energy.

**Acknowledgements** This work is partially supported by National Natural Science Foundation of China (Grants No. 11021092, No. 10975003, No. 11035003, and No. 11120101004), by the Research Fund for the Doctoral Program of Higher Education (China)

## References

1. S. J. Brodsky, F. Fleuret, C. Hadjidakis and J. P. Lansberg, arXiv:1202.6585 [hep-ph].
2. V. Barone, A. Drago and P.G. Ratcliffe, Phys. Rept. **359**, 1 (2002) [arXiv:hep-ph/0104283].
3. R.N. Cahn, Phys. Lett. B **78**, 269 (1978).
4. U. D’Alesio and F. Murgia, Prog. Part. Nucl. Phys. **61**, 394 (2008) [arXiv:0712.4328 [hep-ph]].
5. V. Barone, F. Bradamante and A. Martin, Prog. Part. Nucl. Phys. **65**, 267 (2010) [arXiv:1011.0909 [hep-ph]].
6. D. Boer, M. Diehl, R. Milner, R. Venugopalan, W. Vogelsang, D. Kaplan, H. Montgomery and S. Vignani *et al.*, arXiv:1108.1713 [nucl-th].
7. S. Falciano *et al.* (NA10 Collaboration), Z. Phys. C **31**, 513 (1986).
8. M. Guanziroli *et al.* (NA10 Collaboration), Z. Phys. C **37**, 545 (1988).
9. A. Brandenburg, O. Nachtmann and E. Mirkes, Z. Phys. C **60**, 697 (1993).
10. C.S. Lam and W.K. Tung, Phys. Rev. D **18**, 2447 (1978).
11. C.G. Callan and D.J. Gross, Phys. Rev. Lett. **22**, 156 (1969).
12. J.S. Conway *et al.*, (E615 Collaboration) Phys. Rev. D **39**, 92 (1989).
13. L.Y. Zhu *et al.* (FNAL-E866/NuSea Collaboration), Phys. Rev. Lett. **99**, 082301 (2007) [arXiv:hep-ex/0609005].
14. L.Y. Zhu *et al.* (FNAL E866/NuSea Collaboration), Phys. Rev. Lett. **102**, 182001 (2009) [arXiv:0811.4589 [nucl-ex]].
15. D. L. Adams *et al.* [E581 and E704 Collaborations], Phys. Lett. B **261**, 201 (1991).
16. D. L. Adams *et al.* [E581 and E704 Collaborations], Phys. Lett. B **276**, 531 (1992).
17. D. L. Adams *et al.* [E581 and E704 Collaborations], Z. Phys. C **56**, 181 (1992).
18. D. L. Adams *et al.* [FNAL-E704 Collaboration], Phys. Lett. B **264**, 462 (1991).
19. D. L. Adams *et al.* [FNAL E704 Collaboration], Phys. Rev. D **53**, 4747 (1996).
20. A. Bravar *et al.* [Fermilab E704 Collaboration], Phys. Rev. Lett. **77**, 2626 (1996).
21. A. Bravar [Spin Muon Collaboration], Nucl. Phys. A **666**, 314 (2000).
22. A. Airapetian *et al.* [HERMES Collaboration], Phys. Rev. Lett. **94**, 012002 (2005) [hep-ex/0408013].
23. V. Y. Alexakhin *et al.* [COMPASS Collaboration], Phys. Rev. Lett. **94**, 202002 (2005) [hep-ex/0503002].
24. M. Diefenthaler [HERMES Collaboration], AIP Conf. Proc. **792**, 933 (2005) [hep-ex/0507013].
25. A. Airapetian *et al.* [HERMES Collaboration], Phys. Rev. Lett. **103**, 152002 (2009) [arXiv:0906.3918 [hep-ex]].
26. E. S. Ageev *et al.* [COMPASS Collaboration], Nucl. Phys. B **765**, 31 (2007) [hep-ex/0610068].
27. M. G. Alekseev *et al.* [The COMPASS Collaboration], Phys. Lett. B **692**, 240 (2010) [arXiv:1005.5609 [hep-ex]].
28. G. L. Kane, J. Pumplin and W. Repko, Phys. Rev. Lett. **41**, 1689 (1978).
29. W.J. Stirling and M.R. Whalley, J. Phys. G **19**, D1 (1993).

30. D. Boer, A. Brandenburg, O. Nachtmann and A. Utermann, *Eur. Phys. J. C* **40**, 55 (2005) [arXiv:hep-ph/0411068].
31. A. Brandenburg, S.J. Brodsky, V.V. Khoze and D. Müller, *Phys. Rev. Lett.* **73**, 939 (1994) [arXiv:hep-ph/9403361].
32. K.J. Eskola, P. Hoyer, M. Vanttinen and R. Vogt, *Phys. Lett. B* **333**, 526 (1994) [arXiv:hep-ph/9404322].
33. J.G. Heinrich *et al.*, *Phys. Rev. D* **44**, 1909 (1991).
34. M. Blazek, M. Biyajima and N. Suzuki, *Z. Phys. C* **43**, 447 (1989).
35. D. Boer, *Phys. Rev. D* **60**, 014012 (1999) [arXiv:hep-ph/9902255].
36. P.J. Mulders and R.D. Tangerman, *Nucl. Phys. B* **461**, 197 (1996) [Erratum-*ibid.* **B 484**, 538 (1997)] [arXiv:hep-ph/9510301].
37. D. Boer and P.J. Mulders, *Phys. Rev. D* **57**, 5780 (1998) [arXiv:hep-ph/9711485].
38. Z. Lu and B.-Q. Ma, *Phys. Rev. D* **70**, 094044 (2004) [arXiv:hep-ph/0411043].
39. Z. Lu and B.-Q. Ma, *Phys. Lett. B* **615**, 200 (2005) [arXiv:hep-ph/0504184].
40. A. Bianconi and M. Radici, *Phys. Rev. D* **72**, 074013 (2005) [arXiv:hep-ph/0504261].
41. A.N. Sissakian, O.Y. Shevchenko, A.P. Nagaytsev and O.N. Ivanov, *Phys. Rev. D* **72**, 054027 (2005) [arXiv:hep-ph/0505214].
42. A. Sissakian, O. Shevchenko, A. Nagaytsev, O. Denisov and O. Ivanov, *Eur. Phys. J. C* **46**, 147 (2006) [arXiv:hep-ph/0512095].
43. Z. Lu, B.-Q. Ma and I. Schmidt, *Phys. Lett. B* **639**, 494 (2006) [arXiv:hep-ph/0702006].
44. V. Barone, Z. Lu and B.-Q. Ma, *Eur. Phys. J. C* **49**, 967 (2007) [arXiv:hep-ph/0612350].
45. Z. Lu, B.-Q. Ma and I. Schmidt, *Phys. Rev. D* **75**, 014026 (2007) [arXiv:hep-ph/0701255].
46. L.P. Gamberg and G.R. Goldstein, *Phys. Lett. B* **650**, 362 (2007) [arXiv:hep-ph/0506127].
47. B. Zhang, Z. Lu, B.-Q. Ma and I. Schmidt, *Phys. Rev. D* **77**, 054011 (2008) [arXiv:0803.1692 [hep-ph]].
48. B. Zhang, Z. Lu, B.-Q. Ma and I. Schmidt, *Phys. Rev. D* **78**, 034035 (2008) [arXiv:0807.0503 [hep-ph]].
49. V. Barone, S. Melis and A. Prokudin, *Phys. Rev. D* **82**, 114025 (2010) [arXiv:1009.3423 [hep-ph]].
50. Z. Lu and I. Schmidt, *Phys. Rev. D* **81**, 034023 (2010) [arXiv:0912.2031 [hep-ph]].
51. Z. Lu and I. Schmidt, *Phys. Rev. D* **84**, 094002 (2011) [arXiv:1107.4693 [hep-ph]].
52. F. Yuan, *Phys. Lett. B* **575**, 45 (2003) [arXiv:hep-ph/0308157].
53. B. Pasquini, M. Pincetti and S. Boffi, *Phys. Rev. D* **76**, 034020 (2007) [arXiv:hep-ph/0612094].
54. M. Göckeler *et al.* (QCDSF and UKQCD Collaborations), *Phys. Rev. Lett.* **98**, 222001 (2007) [hep-lat/0612032].
55. M. Burkardt and B. Hannafious, *Phys. Lett. B* **658**, 130 (2008) [arXiv:0705.1573 [hep-ph]].
56. T. Liu and B.-Q. Ma, arXiv:1201.2472 [hep-ph].
57. J. C. Collins, *Nucl. Phys. B* **396**, 161 (1993) [hep-ph/9208213].
58. S. J. Brodsky, D. S. Hwang and I. Schmidt, *Phys. Lett. B* **530**, 99 (2002) [hep-ph/0201296].
59. S. J. Brodsky, D. S. Hwang and I. Schmidt, *Nucl. Phys. B* **642**, 344 (2002) [hep-ph/0206259].
60. R.K. Ellis, W. Furmanski and R. Petronzio, *Nucl. Phys. B* **207**, 1 (1982).
61. A.V. Efremov and A.V. Radyushkin, *Phys. Lett. B* **94**, 245 (1980).
62. J.C. Collins and D.E. Soper, *Nucl. Phys. B* **194**, 445 (1982).
63. X. Ji and F. Yuan, *Phys. Lett. B* **543**, 66 (2002) [arXiv:hep-ph/0206057].
64. A. V. Belitsky, X. Ji and F. Yuan, *Nucl. Phys. B* **656**, 165 (2003) [hep-ph/0208038].
65. D. Boer, P. J. Mulders and F. Pijlman, *Nucl. Phys. B* **667**, 201 (2003) [hep-ph/0303034].
66. J. C. Collins, *Phys. Lett. B* **536**, 43 (2002) [hep-ph/0204004].
67. J. C. Collins and A. Metz, *Phys. Rev. Lett.* **93**, 252001 (2004) [hep-ph/0408249].
68. J. Collins and J. -W. Qiu, *Phys. Rev. D* **75**, 114014 (2007) [arXiv:0705.2141 [hep-ph]].
69. J. Collins, arXiv:0708.4410 [hep-ph].
70. W. Vogelsang and F. Yuan, *Phys. Rev. D* **76**, 094013 (2007) [arXiv:0708.4398 [hep-ph]].
71. C. J. Bomhof and P. J. Mulders, *Nucl. Phys. B* **795**, 409 (2008) [arXiv:0709.1390 [hep-ph]].
72. T. C. Rogers and P. J. Mulders, *Phys. Rev. D* **81**, 094006 (2010) [arXiv:1001.2977 [hep-ph]].
73. J.C. Collins and D.E. Soper, *Phys. Rev. D* **16**, 2219 (1977).
74. E. Mirkes and J. Ohnemus, *Phys. Rev. D* **50**, 5692 (1994) [arXiv:hep-ph/9406381].
75. D. Boer and W. Vogelsang, *Phys. Rev. D* **74**, 014004 (2006) [arXiv:hep-ph/0604177].
76. E.L. Berger, J.W. Qiu and R.A. Rodriguez-Pedraza, *Phys. Lett. B* **656**, 74 (2007) [arXiv:0707.3150 [hep-ph]].
77. E.L. Berger, J.W. Qiu and R.A. Rodriguez-Pedraza, *Phys. Rev. D* **76**, 074006 (2007) [arXiv:0708.0578 [hep-ph]].
78. C. Boros, Z. T. Liang and T. C. Meng, *Phys. Rev. Lett.* **70**, 1751 (1993).
79. D. W. Sivers, *Phys. Rev. D* **41**, 83 (1990).
80. D. W. Sivers, *Phys. Rev. D* **43**, 261 (1991).

- 
81. M. Anselmino, M. Boglione and F. Murgia, Phys. Lett. B **362**, 164 (1995) [hep-ph/9503290].
82. M. Anselmino and F. Murgia, Phys. Lett. B **442**, 470 (1998) [hep-ph/9808426].
83. F. Yuan, Phys. Rev. D **78** (2008) 014024 [arXiv:0801.4357 [hep-ph]].
84. A. Airapetian *et al.* [HERMES Collaboration], Phys. Lett. B **693**, 11 (2010) [arXiv:1006.4221 [hep-ex]].
85. A. Airapetian *et al.* [HERMES Collaboration], Phys. Rev. Lett. **103**, 152002 (2009) [arXiv:0906.3918 [hep-ex]].
86. X. Qian *et al.* [The Jefferson Lab Hall A Collaboration], Phys. Rev. Lett. **107**, 072003 (2011) [arXiv:1106.0363 [nucl-ex]].
87. M. Anselmino, M. Boglione, U. D'Alesio, A. Kotzinian, F. Murgia and A. Prokudin, Phys. Rev. D **72**, 094007 (2005) [Erratum-ibid. D **72**, 099903 (2005)] [hep-ph/0507181].
88. A. V. Efremov, K. Goetze, S. Menzel, A. Metz and P. Schweitzer, Phys. Lett. B **612**, 233 (2005) [hep-ph/0412353].
89. J. C. Collins, A. V. Efremov, K. Goetze, S. Menzel, A. Metz and P. Schweitzer, Phys. Rev. D **73**, 014021 (2006) [hep-ph/0509076].
90. W. Vogelsang and F. Yuan, Phys. Rev. D **72**, 054028 (2005) [hep-ph/0507266].
91. M. Anselmino, M. Boglione, U. D'Alesio, A. Kotzinian, S. Melis, F. Murgia, A. Prokudin and C. Turk, Eur. Phys. J. A **39**, 89 (2009) [arXiv:0805.2677 [hep-ph]].
92. X. -d. Ji, J. -p. Ma and F. Yuan, Phys. Rev. D **71**, 034005 (2005) [hep-ph/0404183].
93. X. -d. Ji, J. -P. Ma and F. Yuan, Phys. Lett. B **597**, 299 (2004) [hep-ph/0405085].
94. M. Anselmino, M. Boglione, U. D'Alesio, A. Kotzinian, F. Murgia, A. Prokudin and C. Turk, Phys. Rev. D **75**, 054032 (2007) [hep-ph/0701006].
95. M. Anselmino, M. Boglione, U. D'Alesio, A. Kotzinian, F. Murgia, A. Prokudin and S. Melis, Nucl. Phys. Proc. Suppl. **191**, 98 (2009) [arXiv:0812.4366 [hep-ph]].
96. V. Barone, S. Melis and A. Prokudin, Phys. Rev. D **81**, 114026 (2010) [arXiv:0912.5194 [hep-ph]].
97. B. Pasquini, S. Cazzaniga and S. Boffi, Phys. Rev. D **78**, 034025 (2008) [arXiv:0806.2298 [hep-ph]].
98. A. Bacchetta, F. Conti and M. Radici, Phys. Rev. D **78**, 074010 (2008) [arXiv:0807.0323 [hep-ph]].
99. H. Avakian, A. V. Efremov, P. Schweitzer and F. Yuan, Phys. Rev. D **78**, 114024 (2008) [arXiv:0805.3355 [hep-ph]].
100. J. She, J. Zhu and B. -Q. Ma, Phys. Rev. D **79**, 054008 (2009) [arXiv:0902.3718 [hep-ph]].
101. A. V. Efremov, P. Schweitzer, O. V. Teryaev and P. Zavada, Phys. Rev. D **80**, 014021 (2009) [arXiv:0903.3490 [hep-ph]].
102. S. Boffi, A. V. Efremov, B. Pasquini and P. Schweitzer, Phys. Rev. D **79**, 094012 (2009) [arXiv:0903.1271 [hep-ph]].
103. H. Avakian, A. V. Efremov, P. Schweitzer and F. Yuan, Phys. Rev. D **81**, 074035 (2010) [arXiv:1001.5467 [hep-ph]].
104. J. Zhu and B. -Q. Ma, Phys. Lett. B **696**, 246 (2011) [arXiv:1104.4564 [hep-ph]].
105. J. Zhu and B. -Q. Ma, Phys. Rev. D **82**, 114022 (2010) [arXiv:1103.4201 [hep-ph]].
106. J. Zhu and B. -Q. Ma, Eur. Phys. J. C **71**, 1807 (2011) [arXiv:1104.5545 [hep-ph]].
107. Z. Lu, B. -Q. Ma and J. Zhu, Phys. Rev. D **84**, 074036 (2011) [arXiv:1108.4974 [hep-ph]].
108. S. Arnold, A. Metz and M. Schlegel, Phys. Rev. D **79**, 034005 (2009) [arXiv:0809.2262 [hep-ph]].
109. A. Bacchetta, M. Boglione, A. Henneman and P. J. Mulders, Phys. Rev. Lett. **85**, 712 (2000) [hep-ph/9912490].
110. E. P. Wigner, Annals Math. **40**, 149 (1939) [Nucl. Phys. Proc. Suppl. **6**, 9 (1989)].
111. H. J. Melosh, Phys. Rev. D **9**, 1095 (1974).
112. B.-Q. Ma, J. Phys. G **17**, L53 (1991) [arXiv:0711.2335 [hep-ph]].
113. B.-Q. Ma and Q.-R. Zhang, Z. Phys. C **58**, 479 (1993)
114. B. -Q. Ma, Phys. Lett. B **375**, 320 (1996) [Erratum-ibid. B **380**, 494 (1996)] [hep-ph/9604423].
115. B. -Q. Ma, I. Schmidt and J. Soffer, Phys. Lett. B **441**, 461 (1998) [hep-ph/9710247].
116. I. Schmidt and J. Soffer, Phys. Lett. B **407**, 331 (1997) [hep-ph/9703411].
117. Z. Lu and B. -Q. Ma, Nucl. Phys. A **741**, 200 (2004) [hep-ph/0406171].
118. B. -Q. Ma, I. Schmidt and J. -J. Yang, Phys. Rev. D **65**, 034010 (2002) [hep-ph/0110324].
119. B. -Q. Ma, I. Schmidt and J. -J. Yang, Phys. Rev. D **66**, 094001 (2002) [hep-ph/0209114].